Electrochimica Acta 196 (2016) 422–430

Contents lists available at ScienceDirect

Electrochimica Acta

journal homepage: www.elsevier.com/locate/electacta

Facile and green fabrication of size-controlled AuNPs/CNFs hybrids for the highly sensitive simultaneous detection of heavy metal ions

Bin Zhang[a], JiaDong Chen[a], Han Zhu[a], TingTing Yang[a], MeiLing Zou[a], Ming Zhang[a,b], MingLiang Du[a,b,*]

[a] Department of Materials Engineering, College of Materials and Textiles, Zhejiang Sci-Tech University, Hangzhou 310018, PR China
[b] Key Laboratory of Advanced Textile Materials and Manufacturing Technology, Zhejiang Sci-Tech University, Ministry of Education, Hangzhou 310018, PR China

ARTICLE INFO

Article history:
Received 9 December 2015
Received in revised form 24 February 2016
Accepted 24 February 2016
Available online 26 February 2016

Keywords:
AuNPs
carbon nanofibers
SWASV
electrochemical detection
heavy metals

ABSTRACT

A well-dispersed Au nanoparticle grown on carbon nanofibers (AuNPs/CNFs) with excellent electroanalytical activity and sensitivity towards the detection of heavy metal ions was synthesized via electrospinning technology and *in situ* thermal reduction. Field-emission scanning electron microscopy (FE-SEM) and transmission electron microscopy (TEM) images show that a large amount of AuNPs with a diameter of 5–15 nm was homogenously distributed on the surface of the nanofibers. The AuNPs/CNFs hybrids modified electrode was utilized as the working electrode for the simultaneous detection of heavy metal ions such as Cd^{2+}, Pb^{2+} and Cu^{2+} through the square wave anodic stripping voltammetry (SWASV) method. The electrochemical results indicate that the simultaneous detection of Cd^{2+}, Pb^{2+} and Cu^{2+} with a low concentration of 0.1 μM can be obtained. This work may provide an easy way to construct electrochemical sensors for the quick detection of trace heavy metal ions.

1. Introduction

Recently, heavy metal pollution, including cadmium, lead and copper, has received great attention due to its high toxicity and easy accumulation. This type of pollution could be seriously hazardous not only to the environment around biological systems but also directly to human beings [1–5]. Therefore, a direct and highly sensitive determination of heavy metallic solutions is of great importance, and huge efforts have been made to achieve efficient methods to realize fast and accurate detection.

With the rapid developments in materials science and technology, *in situ* analysis for tracing heavy metals is highly desired. Although the conventional analytical methods, such as atomic fluorescence spectrometry (AFS) [6], hyper-Rayleigh scattering [7], and inductively-coupled plasma mass spectrometry (ICP-MS) [8], have relatively low detection limits and high precision, the drawbacks of high cost, complicated pre-processing and being limited to single composition detection seriously restrict their widespread application in real-time online and continuous monitoring. Alternatively, the electrochemical analysis method can achieve this due to its portability, high sensitivity, good selectivity, low cost, and suitability, attracting much attention from researchers in the detection field, especially for heavy metal ions.

Currently, square wave anodic stripping voltammetry (SWASV) is widely used for the determination of trace heavy metal ions due to its excellent sensitivity and low detection limits. As one of the electrochemical methods, SWASV has impressive advantages over other voltammetry methods, such as excellent sensitivity, the unique ability to certain metals and the ability to simultaneously analyze several heavy metal ions [9–14]. Typically, SWASV includes two independent procedures: deposition and stripping. First, in the deposition process, metal ions can be reduced under a certain potential from the sample solution to the working electrode. Inversely, when stripping, the reduced metals are oxidized to their ions [15,16]. For the SWASV methods, the ability to dynamically assess low metal concentrations in aqueous solutions is critical for the highly efficient detection of trace heavy metal ions [17]. Consequently, it is of great importance to design fantasy electrode materials, which are essential for the satisfactory performance of electrochemical sensors.

In regard to electrode materials, we can hardly ignore nanomaterials due to their large specific surface area, fast mass transfer speed and countless active sites. Nanomaterials-based sensors exhibit an extremely high surface area, which can increase the

* Corresponding author.
E-mail address: du@zstu.edu.cn (M. Du).

http://dx.doi.org/10.1016/j.electacta.2016.02.163
0013-4686/

number of binding sites available for the adsorption of metal ions [18–21]. Moreover, the unitization of nanomaterials usually leads to faster charge transfer rates, resulting in lower detection limits and faster analyte detection rates than those of conventional sensors [20,22,23]. Large amounts of nanomaterials, such as noble metal nanoparticles (NPs), carbon nanotubes (CNTs) and graphene, have been employed to construct electrochemical sensors [24–27]. Moreover, carbon nanomaterials are becoming more and more popular due to their attractive conductivities, broad potential range, easy modification and low cost. In recent decades, large amounts of carbonaceous materials, such as graphene [28,29], CNTs [30–32], carbon paste, carbon nanospheres [33] and porous carbons [34,35], have been applied to fabricate efficient electrochemical sensors. Several groups have demonstrated sensitive sensors using CNTs [36,37] and graphene [25]. Myung *et al.* fabricated a graphene-encapsulated nanoparticle-based sensor for the selective detection of cancer biomarkers [38]. Chen et al. reported on CNTs-based electrochemical devices for the electronic sensing of protein [39]. In our previous work, size-controlled nanocrystals grown on carbon nanofibers (CNFs) were successfully constructed by combining an electrospinning technology and thermal reduction [40,41]; the as-prepared nanocrystal/CNFs nanostructure was used in the aspects of electrochemical applications related to electrochemical biosensors and electrocatalytic devices [42,43]. CNFs with high length-to-diameter ratio are capable of offering additional active sites for nanoparticle loading or deposition.

To realize a much higher sensitive and selective electroanalysis, many have explored composite-modified electrodes [44], which probably contribute to significantly enhance electrochemical activity. Moreover, the relatively simple and easily synthe sized gold nanoparticles (AuNPs) have been proven to be an excellent material for tracing heavy metals [45,46], which can further improve the response signals in SWASV. Our group has reported electrochemical biosensor designs using noble metal nanostructures for the detection of H_2O_2, glucose and glutathione [43,47,48]. In the present investigation, we propose a new strategy for the design and synthesis of small, size-controlled and well-dispersed AuNPs grown on CNFs. The fabricated AuNPs/CNFs hybrids is used as an electrochemical sensor for the detection of trace heavy metal ions and exhibits a low detection limit and wider response range, indicating its promising potential application in tracing and monitoring low concentrations of heavy metals.

2. Experimental section

2.1. Materials

Chloroauric acid ($HAuCl_4 \cdot 4H_2O$, 99.9%) was acquired from Shanghai Civi Chemical Technology Co., Ltd. Epigallocatechingallate (EGCG) was purchased from Xuancheng Baicao Plant Industry and Trade Co., Ltd. N, N'-dimethylformamide (DMF) was purchased from Shanghai Shenbo Chemical Co., Ltd (China). Phosphate buffer (PB) was obtained from Hangzhou Gaojing Fine Chemical Co. Ltd. Nafion aqueous solution (5 wt%) was obtained from Aldrich Chemistry Co., Ltd. $Pb(NO_3)_2$, $Cd(NO_3)_2 \cdot 4H_2O$, $CuCl_2 \cdot 2H_2O$, $K_3Fe(CN)_6$, KCl and other reagents were purchased from Aladdin Sinopharm Chemical Reagent Co., Ltd. (Shanghai, China). All the chemicals were used as received without further purification. Deionized water (DIW) was used for all solution preparations.

2.2. Apparatus

Transmission electron microscopy (TEM) images were obtained by using a JSM-2100 transmission electron microscope (JEOL, Japan) at an acceleration voltage of 200 kV. The morphologies of the electrospun AuNPs/CNFs hybrids were observed by using a JSM-6700F field-emission scanning electron microscope (FE-SEM, JEOL, Japan) at an acceleration voltage of 3 kV. The X-ray photoelectron spectra of the AuNPs/CNFs hybrids were recorded using an X-ray photoelectron spectrometer (Kratos Axis Ultra DLD) with an aluminum (mono) Kα source (1486.6 eV). The aluminum Kα source was operated at 15 kV and 10 mA. All cyclic electrochemical measurements (cyclic voltammetry and square wave anodic stripping voltammetry (SWASV)) were carried out using a CHI660E computer-controlled potentiostat (ChenHua Instruments Co., Shanghai, China) and performed in a conventional three-electrode cell with either a bare or modified glassy carbon electrodes (GCE) as the working electrode, a platinum electrode as the counter electrode and a saturated calomel electrode (SCE, ChenHua Instruments Co., Shanghai, China) as the reference electrode.

2.3. Preparation of AuNPs in Polyacrylonitrile (PAN) electrospun precursor solution and AuNPs embedded in Polyacrylonitrile nanofibers (AuNPs/PAN)

To prepare the precursor solution, 1.5 g of PAN was first dissolved in 10 mL of DMF under moderate stirring to obtain a homogeneous solution. Then, the mixtures were poured into a conical flask (fitted with a reflux condenser and a Teflon-coated stir bar) and heated to 60 °C, with vigorous stirring by magnetic force. After a while, Au (III) solution was added into the 3-neck flask by dripping slowly. In the last step, 0.0125 g of EGCG, dissolved in 5 mL of DMF, was injected into the above Au mixture solution after a homogeneous solution was obtained. Within this condition, vigorous stirring was continued until the mixture was uniform, thus producing the precursor solution.

The electrospun procedure of the AuNPs/PAN precursor was the same as for the PAN nanofibers. The feed rate, voltage and distance were 0.6 mL/h, 15 kV and 15 cm, respectively. All experiments were performed at room temperature. The electrospun AuNPs/PAN nanofibrous mats were collected onto a scroll wheel and then preserved through drying for further use.

2.4. Preparation of size-controlled AuNPs in carbon nanofibers (AuNPs/CNFs) hybrids

First, a piece of an electrospun AuNPs nanofibrous mat (10 × 15 mm) was put into a homemade chemical vapor deposition (CVD) tube furnace for heat treatment and then heated at 300 °C in air for the first stage; the corresponding heating rate was 5 °C/min. Then, the samples were heated to 900 °C for graphitization for 6 h in Ar (120 Sccm) gas flow. Finally, the samples were held at the desired graphitization temperature for 4 h to gain full carbonization and subsequently cooled to room temperature under an Ar atmosphere.

2.5. Preparation of AuNPs/CNFs modified GCE (AuNPs/CNFs/GCE)

The bare GCE was ultrasonically processed in ethanol for 20 min to reduce the surface residue and then polished carefully with 0.3 and 0.05 μm of alumina slurry, followed by rinsing in ethanol and doubly distilled water and then drying. 3 mg of AuNPs/CNFs powder was dispersed in 1 mL of mixture solvent, composed of 3:1 (v/v) isopropanol/distilled water and 30 μL of Nafion solution (5 wt %) by ultrasonication to form a homogeneous ink. Additionally, 5 μL of ink was carefully transferred onto the GCE and dried at room temperature. The modified electrode is denoted as AuNPs/CNFs/GCE. After solvent evaporation, the electrodes were stored in a desiccator at room temperature before further characterization.

2.6. Simultaneous detection of Cd^{2+}, Pb^{2+}, Cu^{2+} and optimization parameters

Square wave anodic stripping voltammetry (SWASV) was used for the simultaneous detection of Cd^{2+}, Pb^{2+}, and Cu^{2+} on a CHI660E electrochemical workstation. All electrochemical measurements were performed with a three electrode system: the modified GCE (AuNPs/CNFs/GCE) as the working electrode, a platinum electrode as the counter electrode and a saturated calomel electrode (SCE) as the reference electrode. First, the AuNPs/CNFs/GCE electrode was immersed into the mixed liquor containing 0.1 mol L^{-1} of Phosphate Buffer solution (PBS) and metal ions solution. Then, metals were deposited onto the surface of the modified electrode at the potential of −1.8 V vs SCE for 150 s. Briefly, the deposition process was realized via the reduction of corresponding heavy metal ions in the mixture solutions, followed by another invertible process: stripping. All the experiments were carried out under the following experimental conditions: the scanning potential ranged from −1.2 to 0.8 V; the amplitude was 50 mV; the increment potential was 4 mV; the frequency was 15 Hz. Moreover, other external conditions were controlled to ensure the comparability of each experiment. A positive potential was applied to the working electrode for 60 s to remove the deposited residual species from the surface after each detection test.

To gain maximum sensitivity and the minimum limit of detection with the modified electrode (AuNPs/CNFs/GCE), the corresponding voltammetric parameters (deposition potential and deposition time) were optimized via repeated experiments under similar conditions.

3. Results and Discussion

3.1. Morphology of AuNPs/CNFs hybrids

The AuNPs/CNFs hybrids were synthesized according to our previous work [41]. First, AuNPs/PAN nanofibers with homogeneously distributed AuNPs were obtained via an *in situ* reduction and electrospinning procedure. Then, the AuNPs underwent migration from inside to the surface of carbon nanofibers, with the condition of high temperature carbonization. Fig. 1a and b show the FE-SEM images of the as-prepared AuNPs/CNFs. The diameter of the nanofibers was approximately 342 ± 36 nm, and a large amount of AuNPs was homogenously distributed on the surface of the nanofibers. The size-controlled AuNPs were loaded onto the carbon fibers homogenously, which can be further confirmed from the TEM image shown in Fig. 1c. A typical HRTEM image of the AuNPs is shown in Fig. 1d, indicating the lattice fringes of the as-prepared AuNPs. The latter fringe spacing of the AuNPs was approximately 0.217 nm, corresponding to the (111) plane. Moreover, the diameter of the AuNPs was between 5 and 15 nm, as shown in Fig. 1e, which suggests that the AuNPs from our work had smaller size compared with those synthesized using other methods, e.g., the laser ablation in liquid (LAL) method [45], probably contributing to the much higher electrochemical activity

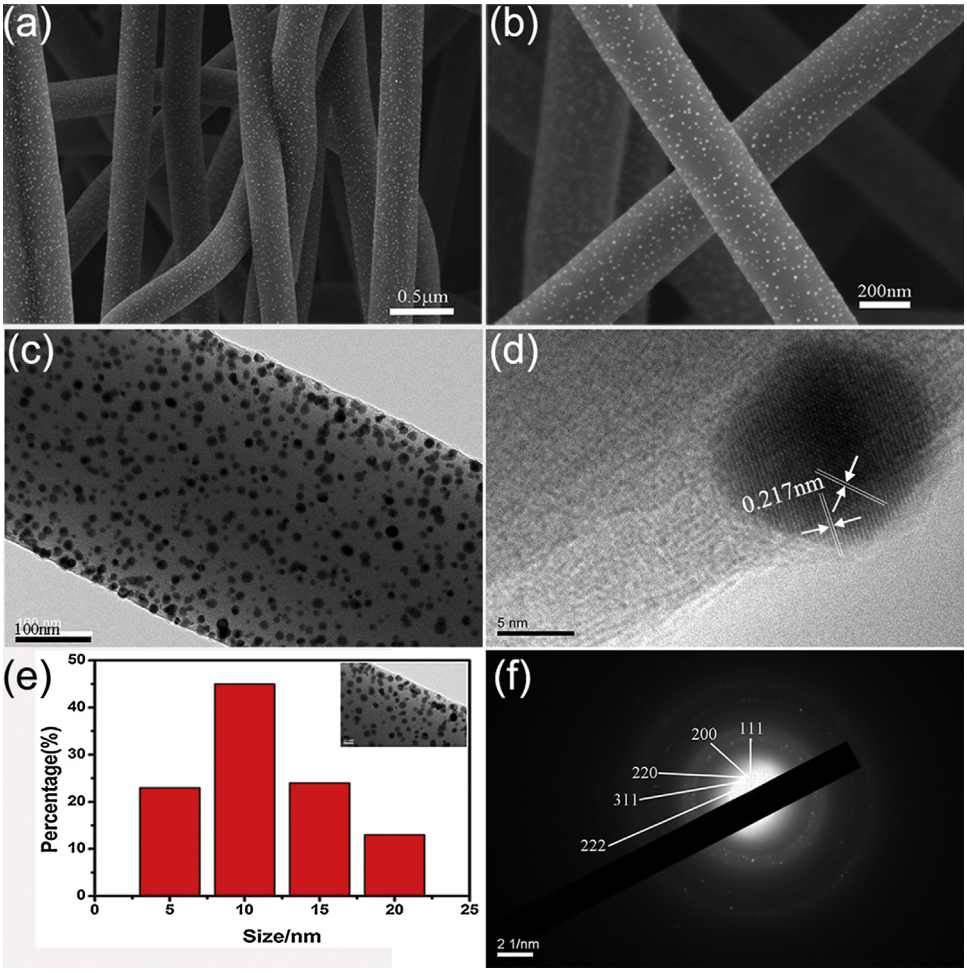

Fig. 1. (a) and (b) FE-SEM images of the different sizes of prepared AuNPs/CNFs via an *in situ* reduction approach. (c) TEM image of the AuNPs/CNFs. (d) HRTEM image of the AuNPs/CNFs. (e) the size distribution of the AuNPs loaded on CNFs; the inset is the corresponding area of the selected AuNPs/CNFs. (f) SAED pattern of the AuNPs/CNFs.

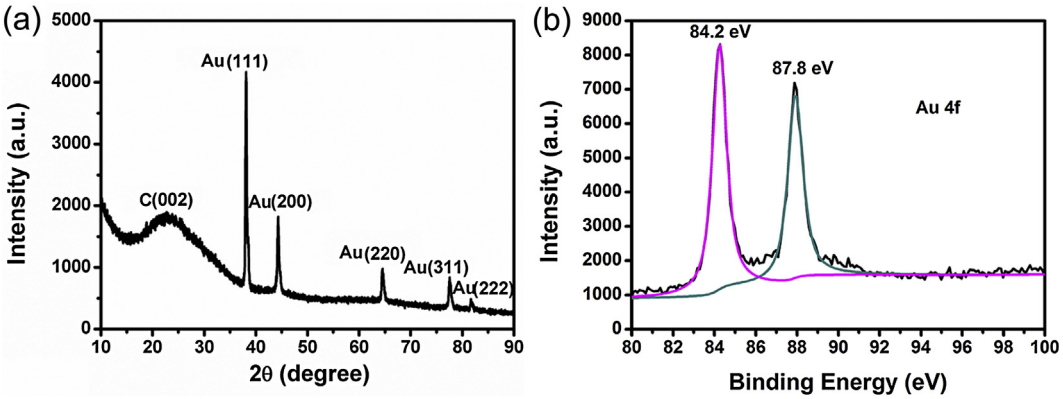

Fig. 2. (a) XRD pattern of the AuNPs/CNFs hybrids. (b) XPS spectrum of Au 4f of the AuNPs/CNFs hybrids.

in the electrochemical characterization. The selected area electron diffraction pattern was consistent with a typical gold crystal and previous results (see Fig. 1f) and the concentric diffraction rings were included the (111), (200), (220), (311) and (222) planes of the Au crystal, from the inside to outside.

As shown in Fig. 2a, a typical diffraction peak of Au crystal emerged on the XRD pattern. The strong representative diffraction peaks appeared at 38.3°, 44.4°, 64.8°, 77.8° and 82.6°, which are consistent with the (111), (200), (220), (311) and (222) planes of the Au crystal. The strong and sharp peaks in Fig. 2a suggest the fantasy crystallization of AuNPs by our method. Moreover, a broad diffraction peak was detected at $2\theta = 24.7°$, indicating the crystalline structure of the graphitic carbon in the nanofibers, which is ascribed to the PAN crystalline phase of the (120) plane and amorphous phase. Meanwhile, the XPS spectrum of the AuNPs/CNFs hybrids is shown in Fig. 2b. Clearly, two sharp and identifiable peaks can be observed at 87.8 and 84.2 eV, respectively, which are associated with the binding energies of Au $4f_{7/2}$ and Au $4f_{5/2}$. The intensity of the Au 4f peaks of AuNPs/CNFs was much higher, indicating that the AuNPs/CNFs had more exposed AuNPs on the surfaces of the carbon nanofibers according to previous research. The XPS results are consistent with the FE-SEM, STEM and XRD results.

The red square in Fig. 3a is the mapping region of the AuNPs/CNFs, which further verified the polycrystalline and face-centered cubic-phase nanocrystalline structure of AuNPs. To further investigate and verify the specific composition elements, we obtained the EDX spectrum of the AuNPs/CNFs hybrids. Fig. 3a shows the C, O and Au elements, proving the presence of AuNPs. Moreover, the HAADF-STEM and STEM-EDS mapping images of CNFs clearly show three typical elements, which are ascribed to carbon, oxygen and nitrogen. We also obtained line-scanned EDX spectra from 3 AuNPs in individual carbon nanofibers, as shown in Fig. 3b and c. The emergent position of gold element was relatively

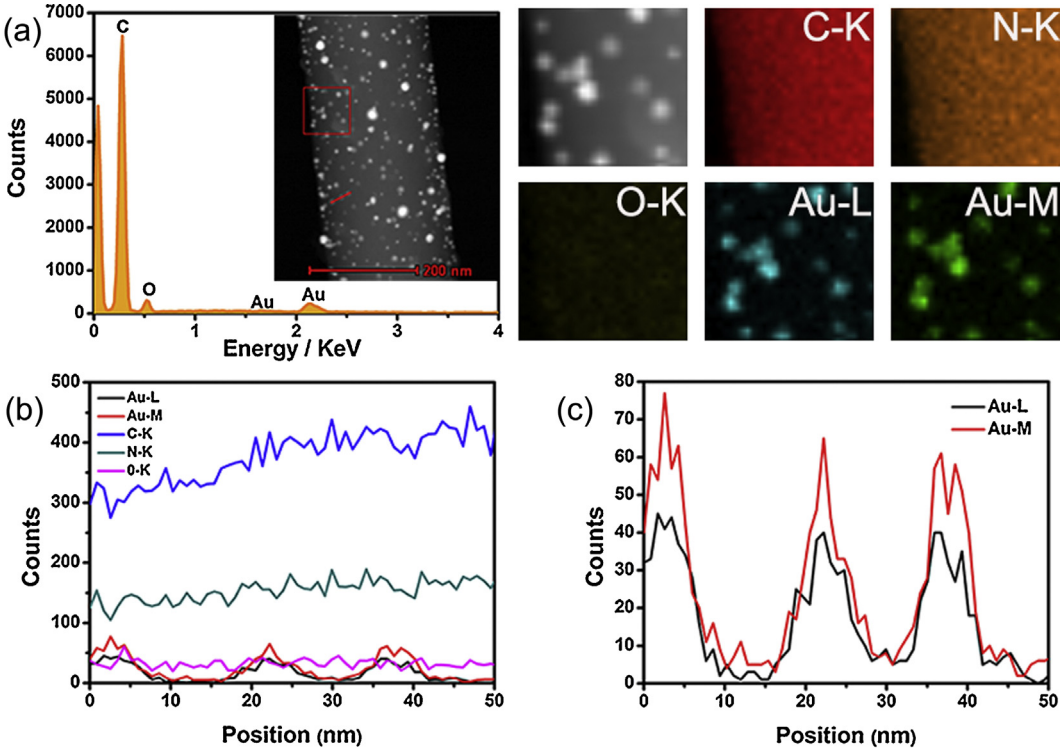

Fig. 3. (a) EDX spectrum of the AuNPs/CNFs hybrids; the inset is an HAADF-STEM image of the AuNPs/CNFs hybrids, and the corresponding STEM-EDS mapping images of the selective area are adjacent to the right. (b) Line scan EDX spectra of the AuNPs/CNFs hybrids for all elements and (c) only for gold. (For interpretation of the references to color in text, the reader is referred to the web version of this article.)

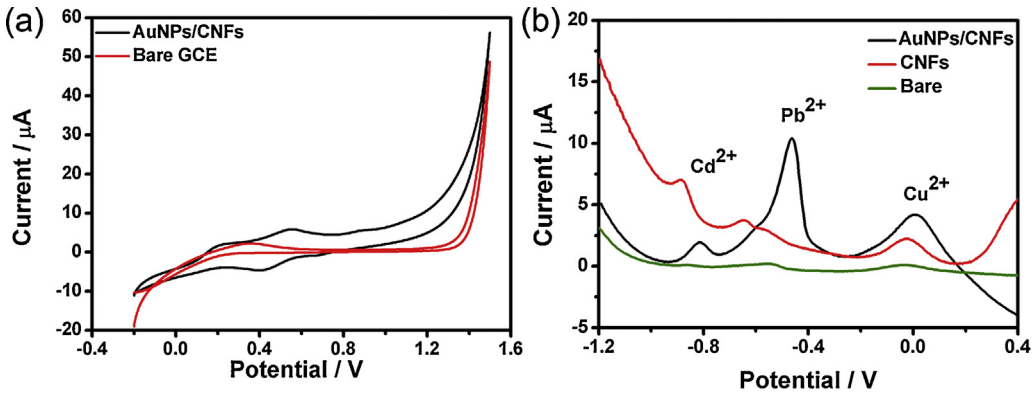

Fig. 4. (a) Cyclic voltammograms response of bare and AuNPs/CNFs hybrids-modified GCE in a solution of 5 mM $K_3[Fe(CN)_6]$, with steps from −0.2 to 1.5 V vs SCE. (b) SWASVs for simultaneous detection of Cd^{2+}, Pb^{2+} and Cu^{2+} with the modified AuNPs/CNFs/GCE, CNFs/GCE and bare/GCE. The conditions are as follows: the concentration of Cd^{2+}, Pb^{2+} and Cu^{2+} is 1 μM, pH 6.8, deposition potential −1.8 V, room temperature, amplitude 50 mV, increment potential 4 mV, frequency 15 Hz.

similar to the ideal position, indicating the existence of gold, carbon, oxygen and nitrogen.

3.2. Electrochemical performance of the AuNPs/CNFs hybrids modified electrode

To fully investigate the electrochemical performance of the GCE modified with our nanomaterials, we performed a series of experiments on the electrode using a cyclic voltammogram (CV) and SWASV. Fig. 4a shows the CV signals of the bare and modified GCE, corresponding to the red and black lines in the figure, which were immersed in a neutral solution of 5 mM $K_3[Fe(CN)_6]$. The CV curves were determined in the potential range from −0.2 to 1.5 V (vs. SCE), with a scan rate of 100 mV/s. Compared with the bare GCE, the modified GCE had a relatively higher peak current and a couple of well-defined oxidation and reduction peaks. This may be ascribed to the existence of modified materials, contributing to the acceleration of the electron transfer process. As a result, the prepared AuNPs/CNFs hybrids exhibit high activity in electron transfer, and the AuNPs/CNFs/GCE possess much better electrochemical catalytic behavior. Fig. 4b shows the SWASV signals of the bare and modified GCE in 1 μM. Compared with the bare GCE, the modified GCE exhibit three well defined peaks of Cd^{2+}, Pb^{2+} and Cu^{2+} with higher current and possess a stable base line, which indicate that the modified AuNPs/CNFs/GCE exhibits excellent electroanalysis capability for simultaneous detection of heavy metal ions.

Fig. 5 demonstrates the SWASV analytical characteristics of the modified GCE. In general, the signals of the stripping peak improve with increasing deposition time and concentration of metal ions, as does the consistency and reproducibility. The stripping currents

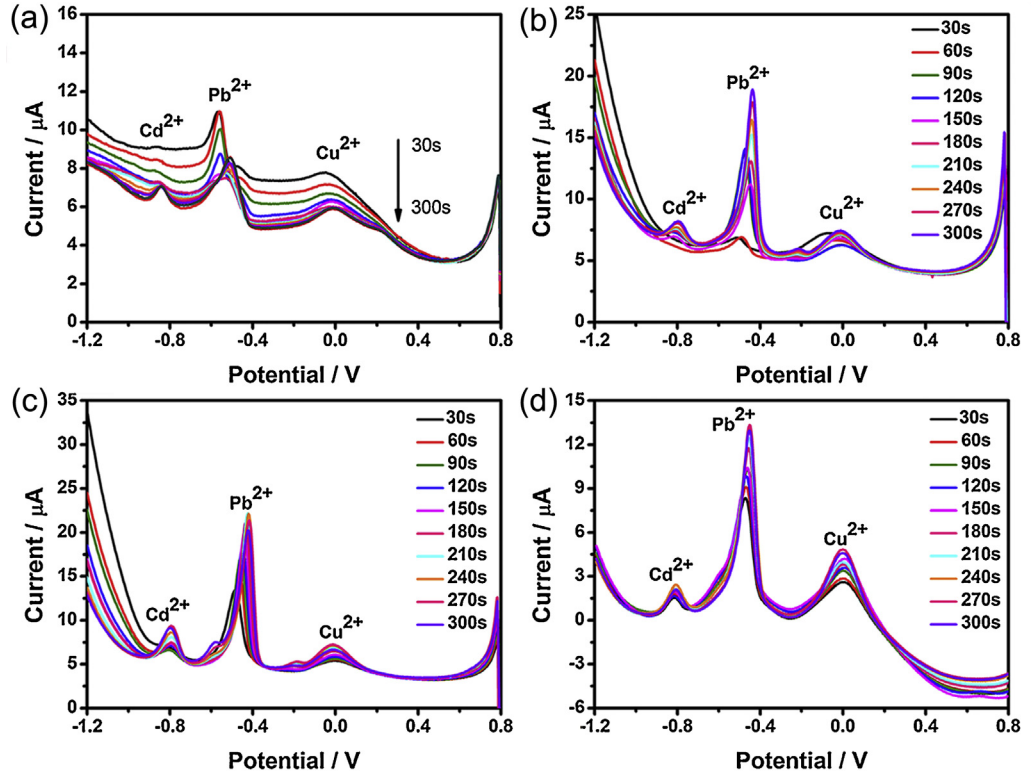

Fig. 5. SWASVs for simultaneous detection of Cd^{2+}, Pb^{2+} and Cu^{2+} over a deposition time range from 30–300 s on AuNPs/CNFs/GCE in 0.1 M PBS and different concentrations of metal ion solution: (a) 0.1 μM, (b) 0.25 μM, (c) 0.5 μM, (d) 1.0 μM. The other experimental conditions are the same as those in Fig. 4.

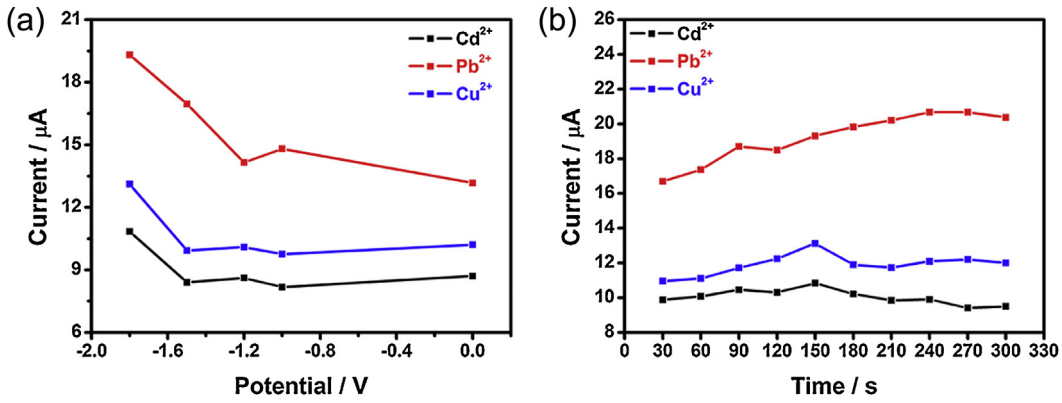

Fig. 6. The experimental parameter deposition potential and deposition time optimization. All data were captured through SWASV detection of a metal ion solution containing 1.0 μM each of Cd^{2+}, Pb^{2+} and Cu^{2+}. The other experimental conditions are the same as those in Fig. 4.

still had good peaks with the modified AuNPs/CNFs electrode, even at such a low concentration (0.1 μM) of metal ions, suggesting that it is suitable for AuNPs/CNFs/GCE as the working electrode to accumulate Cd^{2+}, $Pb^{2+}$and Cu^{2+} and to be stripped at the corresponding potentials.

3.3. Electrochemical experimental parameter optimization of the AuNPs/CNFs hybrids modified electrode

In addition to detecting heavy metal ions with relatively high accuracy, the modified GCE needs to achieve maximum sensitivity for practical application. Thus, optimizing the experimental parameters to obtain an apparent signal is of great importance. Fig. 6 shows the effects of deposition potential and deposition time on the stripping current of the modified GCE. All the experiments were performed in a mixed solution, with 1.0 μM each of Cd^{2+}, Pb^{2+} and Cu^{2+}, under the same controlled conditions. The deposition potential plays a key role in ion accumulation, which mostly decides whether accumulation and reduction are sufficient. Fig. 6a demonstrates that the stripping currents of Cd^{2+}, Pb^{2+} and Cu^{2+} are the highest and show an impressive signal when the deposition potential is at −1.8 V, which is attributed to the full accumulation at this potential for all the metal ions. Therefore, we chose −1.8 V as the optimal deposition potential for the following optimization. The deposition time is also a significant factor that could have a great impact on the sensitivity. Fig. 6b illustrates the stripping current of the 3 target metals, with varying deposition time. For Pb^{2+}, as time increased, the peak current became higher, from 30 to 240 s and then followed a descending trend. Meanwhile, the peak currents of Cu^{2+} and Cd^{2+} exhibited a slight increase as the deposition time increased to 150 s. Then, after a slight decrease, the stripping current remained stable. Based on the optimal deposition time of all metals, 150 s was chosen as the optimum deposition time.

Fig. 7 describes the SWASVs of AuNPs/CNFs/GCE in a mixed solution containing different concentrations of Cd^{2+}, Pb^{2+} and Cu^{2+}. The curves exhibited three obvious signals at the potentials of −0.8, −0.5, and 0 V, corresponding to the oxidation potentials of Cd, Pb and Cu, respectively. Moreover, the stripping peaks exhibited well-defined and well-separated signals for each other, indicating that the modified electrode can simultaneously detect the three target ions as the working electrode at such a low concentration as 0.1 μM. Meanwhile, the excellent sensibility and distinguishability of the modified electrode also indicates that it can be used in the field of practical application effectively.

To investigate the line range of detection, we determined the relationship between the fitting curve of the currents and the concentration of metal ions in Fig. 8. The linearization curve reflects that the currents became higher with increasing ion concentration, ascribed to the aggravation of ion exchange. Fig. 8a, b and c show that the calibration curves were linear over the range from 0.1 to 1.0 μM for the 3 metal ions; the linearization equations are displayed in the figure with the correlation coefficients of 0.973, 0.936 and 0.833, corresponding to Cd^{2+}, Pb^{2+} and Cu^{2+}, respectively. From Table 1, the relative standard deviations (RSD) of the as-prepared sensor for each ion were measured with 5 replicate

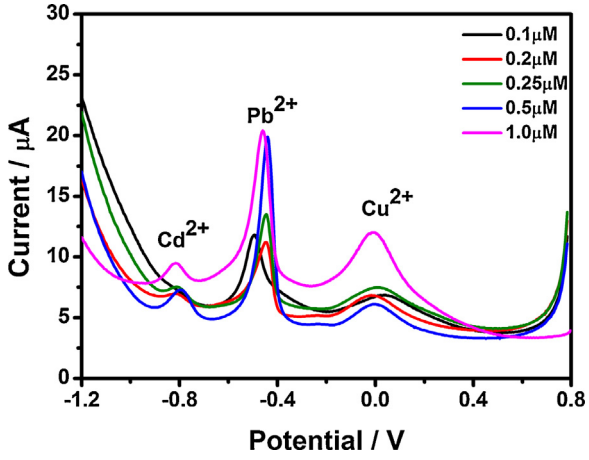

Fig. 7. SWASVs for the simultaneous detection of Cd^{2+}, Pb^{2+} and Cu^{2+} under the optimum conditions. The detection was carried out over a concentration range from 0.1 to 1.0 μM on AuNPs/CNFs/GCE.

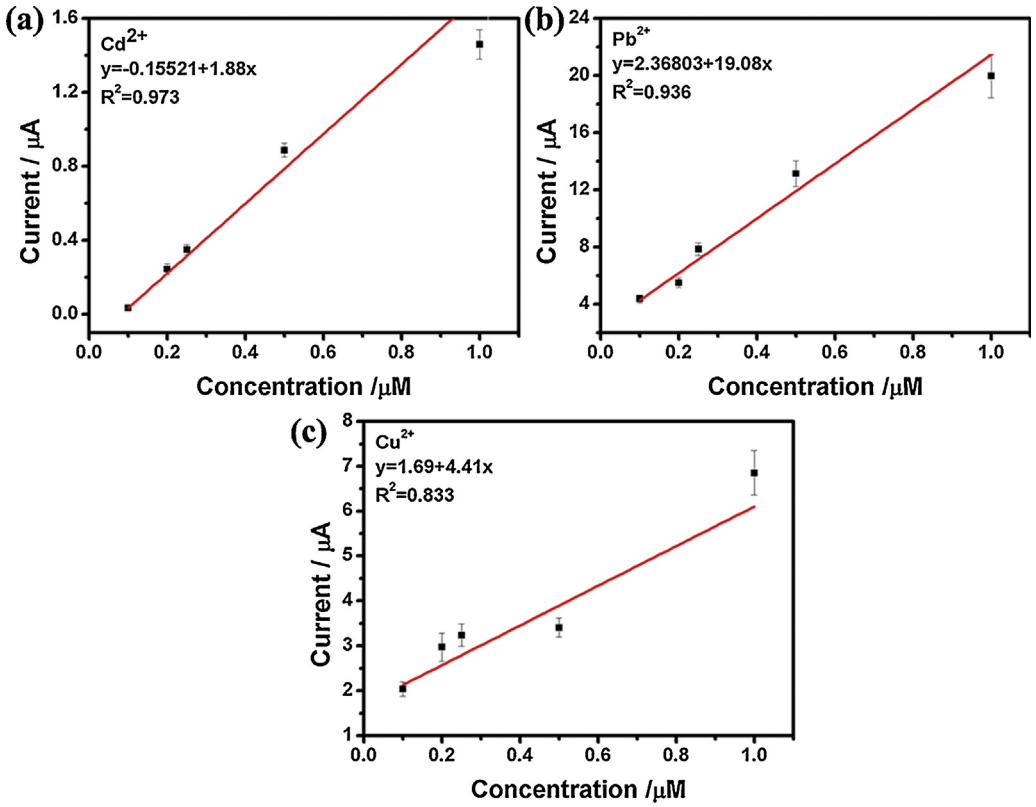

Fig. 8. The corresponding calibration curve plots of Cd^{2+}, Pb^{2+} and Cu^{2+}.

Table 1
The repeatability of as-prepared AuNPs/CNFs.

concentration	RSD[a] for Cd^{2+}	RSD for Pb^{2+}	RSD for Cu^{2+}
0.5 μM	4.27%	6.81%	6.30%
1.0 μM	5.52%	7.61%	7.25%

[a] RSD means the relative standard deviations.

experiments, which indicate the sensor can be applied to detect heavy metal ions simultaneously with high repeatability. Therefore, we can draw the conclusion that Cd^{2+}, Pb^{2+} and Cu^{2+} can be detected simultaneously; the lowest detection concentration reached in our experiments was an incredible 0.1 μM. As a comparison, we list some reported typical electrode materials for the simultaneous detection of Cd^{2+}, Pb^{2+} and Cu^{2+}. From Table 2, it

Table 2
Comparison of some electrode materials for the simultaneous detection of Cd^{2+}, Pb^{2+} and Cu^{2+}.

Electrode materials	method	LD[a] (μmol L^{-1})	Deposition time (s)	Reference
Carbon Nanotube Thread	SWASV	Cd 1.0 Pb 0.25 Cu 0.5	120	[49]
Ti/TiO_2	ASV	Cd 0.6 Pb 0.6 Cu 0.6	300	[50]
$Mo_6S_{9-x}I_x$ Nanowires	DPASV	Cd 0.00445 Pb 0.00724 Cu 0.0126	240	[51]
SnO_2/Reduced Graphene Oxide Nanocomposite	SWASV	Cd 0.3 Pb 0.3 Cu 0.3	120	[10]
AuNPs by LAL	DPASV	Cd 0.3 Pb 0.3 Cu 0.3	300	[45]
AuNPs/CNFs	SWASV	Cd 0.1 Pb 0.1 Cu 0.1	150	This work

[a] the lowest detection concentration for simultaneous detection of Cd^{2+}, Pb^{2+} and Cu^{2+}.

can be seen that the present fabricated AuNPs/CNFs hybrid relative high efficient simultaneous detection of Cd^{2+}, Pb^{2+} and Cu^{2+}.

As a chemical sensor for heavy metal ions, the as-prepared AuNPs/CNFs hybrids demonstrates excellent electrochemical activity, which can be ascribed to the following reasons: (1) the well-dispersed AuNPs fabricated by using the *in-situ* reduction method exhibited favorable electron response to the concentration of metal ions. Moreover, the fabricated AuNPs were much smaller than those reported by other methods [45,46], which may offer a larger surface area for the deposition of metal ions, contributing to the enhancement and separation of electrochemical signals to each other. (2) The high electron transport capability of CNFs also facilitates the stripping and deposition of heavy metal ions; the excellent stability will endow the electrode with good durability. (3) The AuNPs/CNFs hybrids was synthesized via an electrospinning technique and exhibited a high surface-specific area and high porosity, which are beneficial for the penetration of heavy metal ion solutions and increase the surface contact area of the electrode. Moreover, only the chemical reagent EGCG was used for the reduction of AuNPs in the experiments; hence, the present investigation offers a facile, green, highly sensitive and simultaneous method for the detection of trace heavy metal ions.

4. Conclusions

A facile, green, highly sensitive and simultaneous method for the detection of trace heavy metal ions was demonstrated. Well-dispersed AuNPs, grown on carbon nanofibers (AuNPs/CNFs) with excellent electroanalytical activity and sensitivity towards the detection of heavy metal ions, were synthesized via electrospinning technology and *in situ* thermal reduction. The AuNPs/CNFs hybrids modified electrode was utilized as the working electrode for the simultaneous determination of heavy metal ions such as Cd^{2+}, Pb^{2+} and Cu^{2+} through the SWASV method. The electrochemical results indicate that the AuNPs/CNFs hybrids electrode exhibits high sensitivity and a low detection limit of the simultaneous detection of Cd^{2+}, Pb^{2+} and Cu^{2+}, which was attributed to the exposed well-dispersed AuNPs, the high electron transport capability of CNFs, and the high surface-specific area and high porosity of the AuNPs/CNFs hybrids. The present investigation offers an effective and promising method for the simultaneous detection of trace heavy metal ions.

Acknowledgments

This study was supported by the National Natural Science Foundation of China (NSFC) (Grant no. 51373154, 51573166), Program for Innovative Research Team of Zhejiang Sci-Tech University and the 521 Talent Project of Zhejiang Sci-Tech University.

References

[1] J.G. Wiener, D.P. Krabbenhoft, G.H. Heinz, A.M. Scheuhammer, Ecotoxicology of mercury, Handbook of Ecotoxicology 2 (2003) 409.
[2] I.A. Darwish, D.A. Blake, Development and validation of a one-step immunoassay for determination of cadmium in human serum, Analytical Chemistry 74 (2002) 52.
[3] F.B. Edward, C.K. Yap, A. Ismail, S.G. Tan, Interspecific variation of heavy metal concentrations in the different parts of tropical intertidal bivalves, Water, Air and Soil Pollution 196 (2009) 297.
[4] R. Khlifi, A. Hamza-chaffai, Head and neck cancer due to heavy metal exposure via tobacco smoking and professional exposure: A review, Toxicology and Applied Pharmacology 248 (2010) 71.
[5] S.K. Yadav, Heavy metals toxicity in plants: an overview on the role of glutathione and phytochelatins in heavy metal stress tolerance of plants, South African Journal of Botany 76 (2010) 167.
[6] Z. Wan, Z. Xu, J. Wang, Flow injection on-line solid phase extraction for ultra-trace lead screening with hydride generation atomic fluorescence spectrometry, Analyst 131 (2006) 141.
[7] Y. Kim, R.C. Johnson, J.T. Hupp, Gold Nanoparticle-Based Sensing of Spectroscopically Silent Heavy Metal Ions, Nano Letters 1 (2001) 165.
[8] H. Liu, S. Jiang, S. Liu, Determination of cadmium, mercury and lead in seawater by electrothermal vaporization isotope dilution inductively coupled plasma mass spectrometry, Spectrochimica ACTA Part B: Atomic Spectroscopy 54 (1999) 1367.
[9] M.R. Rahman, T. Okajima, T. Ohsaka, Selective detection of As(III) at the Au(III)-like polycrystalline gold electrode, Analytical Chemistry 82 (2010) 9169.
[10] Y. Wei, C. Gao, F. Meng, H. Li, L. Wang, J. Liu, X. Huang, SnO_2 Reduced Graphene Oxide Nanocomposite for the Simultaneous Electrochemical Detection of Cadmium(II) Lead(II), Copper(II), and Mercury(II): An Interesting Favorable Mutual Interference, Journal of Physical Chemistry C 116 (2012) 1034.
[11] Y.B. Mollamahale, M. Ghorbani, M. Ghalkhani, M. Vossoughi, A. Dolati, Highly sensitive 3D gold nanotube ensembles: Application to electrochemical determination of metronidazole, Electrochimica Acta 106 (2013) 288.
[12] R.X. Xu, X.Y. Yu, C. Gao, Y.J. Jiang, D.D. Han, J.H. Liu, X.J. Huang, Non-conductive nanomaterial enhanced electrochemical response in stripping voltammetry: the use of nanostructured magnesium silicate hollow spheres for heavy metal ions detection, Analytica chimica acta 790 (2013) 31.
[13] X. Dai, O. Nekrassova, M.E. Hyde, R.G. Compton, Anodic Stripping Voltammetry of Arsenic(III) Using Gold Nanoparticle-Modified Electrodes, Analytical Chemistry 76 (2004) 5924.
[14] B.K. jena, C.R. raj, Gold Nanoelectrode Ensembles for the Simultaneous Electrochemical Detection of Ultratrace Arsenic Mercury, and Copper, Analytical Chemistry 80 (2008) 4836.
[15] J.B. Jia, L.Y. Cao, Z.H. Wang, T.X. Wang, Properties of Poly (sodium 4-styrenesulfonate)-Ionic Liquid Composite Film and Its Application in the Determination of Trace Metals Combined with Bismuth Film Electrode, Electroanalysis 20 (2008) 542.
[16] E.P. Achterberg, C. Braungardt, Stripping voltammetry for the determination of trace metal speciation and in-situ measurements of trace metal distributions in marine waters, Analytica chimica acta 400 (1999) 381.
[17] P. Pathirathna, Y. Yang, K. Forzley, S.P. Mcelmurry, P. Hashemi, Fast-Scan Deposition-Stripping Voltammetry at Carbon-Fiber Microelectrodes: Real-Time Subsecond, Mercury Free Measurements of Copper, Analytical Chemistry 84 (2012) 6298.
[18] C. Marichy, M. Bechelany, N. Pinna, Atomic layer deposition of nanostructured materials for energy and environmental applications, Advanced Materials 24 (2012) 1017.
[19] L. Matlock-colangelo, A.J. Baeumner, Recent progress in the design of nanofiber-based biosensing devices, Lab on a Chip 12 (2012) 2612.
[20] Y.Q. Wang, B. Yan, L.X. Chen, SERS tags: novel optical nanoprobes for bioanalysis, Chemical Reviews 113 (2012) 1391.
[21] L.N. Cella, W. Chen, N.V. Myung, A. Mulchandani, Single-walled carbon nanotube-based chemiresistive affinity biosensors for small molecules: ultrasensitive glucose detection, Journal of the American Chemical Society 132 (2010) 5024.
[22] X.M. Feng, R.M. Li, Y.W. Ma, R.F. Chen, N.E. Shi, Q.L. Fan, W. Huang, One-Step Electrochemical Synthesis of Graphene/Polyaniline Composite Film and Its Applications, Advanced Functional Materials 21 (2011) 2989.
[23] Y.D. Jin, Engineering Plasmonic Gold Nanostructures and Metamaterials for Biosensing and Nanomedicine, Advanced Materials 24 (2012) 5153.
[24] H. Im, X.J. Huang, B. Gu, Y.K. Choi, A dielectric-modulated field-effect transistor for biosensing, Nature Nanotechnology 2 (2007) 430.
[25] J. Lu, I. Do, L.T. Drzal, R.M. Worden, I. Lee, Nanometal-Decorated Exfoliated Graphite Nanoplatelet Based Glucose Biosensors with High Sensitivity and Fast Response, ACS Nano 2 (2008) 1183.
[26] N.J. Ronkainen, H.B. Halsall, W.R. Heineman, Electrochemical biosensors, Chemical Society Reviews 39 (2010) 1747.
[27] J. Wang, Electrochemical Glucose Biosensors, Chemical Reviews 108 (2008) 814.
[28] Y.Y. Shao, J. Wang, H. Wu, J. Liu, I. Aksay, Y. Lin, Graphene Based Electrochemical Sensors and Biosensors: A Review, Electroanalysis 22 (2010) 1027.
[29] J. Li, S. Guo, Y.M. Zhai, E.K. Wang, Nafion-graphene nanocomposite film as enhanced sensing platform for ultrasensitive determination of cadmium, Electrochemistry Communications 11 (2009) 1085.
[30] M.M. Radhi, W.T. Tan, M. Zaki, B.A. rahman, A.B. Kassim, Voltammetric detection of Hg(II) at C_{60}, activated carbon and MWCNT modified glassy carbon electrode, Research Journal of Applied Sciences 5 (2010) 59.
[31] J. Wang, S.B. Hocevar, B. Ogorevc, Carbon nanotube-modified glassy carbon electrode for adsorptive stripping voltammetric detection of ultratrace levels of 2,4,6-trinitrotoluene, Electrochemistry Communications 6 (2004) 176.
[32] Y. Liu, Y. Li, X. Yan, Preparation, characterization, and application of L-cysteine functionalized multiwalled carbon nanotubes as a selective sorbent for separation and preconcentration of heavy metals, Advanced Functional Materials 18 (2008) 1536.
[33] X.L. Nie, W.B. Hu, Fabrication of a carbon sphere-modified electrode and sensitive determination of cadmium(II), Analytical Sciences 26 (2010) 141.
[34] A. Stein, Z. Wang, M.A. Fierke, Functionalization of Porous Carbon Materials with Designed Pore Architecture, Advanced Materials 21 (2009) 265.
[35] L.S. Zhang, W. Li, Z.M. Cui, W.G. Song, Synthesis of porous and graphitic carbon for electrochemical detection, Journal of Physical Chemistry C 113 (2009) 20594.
[36] J. Morton, N. Havens, A. Mugweru, A.K. Wanekaya, Detection of Trace Heavy Metal Ions Using Carbon Nanotube-Modified Electrodes, Electroanalysis 21 (2009) 1597.

[37] A. Afkhami, H. Ghaedi, T. Madrakian, M. Rezaeivala, Highly sensitive simultaneous electrochemical determination of trace amounts of Pb(II) and Cd (II) using a carbon paste electrode modified with multi-walled carbon nanotubes and a newly synthesized Schiff base, Electrochimica Acta 89 (2013) 377.
[38] S. Myung, A. Solanki, C. Kim, J. Park, K.S. Kim, K. Lee, Graphene-Encapsulated Nanoparticle-Based Biosensor for the Selective Detection of Cancer Biomarkers, Advanced Materials 23 (2011) 2221.
[39] R.J. Chen, H.C. Choi, S. Bangsaruntip, E. Yenilmez, X.W. Tang, Q. Wang, Y.L. Chang, H.J. Dai, An Investigation of the Mechanisms of Electronic Sensing of Protein Adsorption on Carbon Nanotube Devices, Journal of the American Chemical Society 126 (2004) 1563.
[40] M.L. Zou, M.L. Du, H. Zhu, C. Xu, N. Li, Y. Fu, Synthesis of silver nanoparticles in electrospun polyacrylonitrile nanofibers using tea polyphenols as the reductant, Polymer Engineering & Science 53 (2013) 1099.
[41] H. Zhu, M. Du, M. Zhang, M. Zou, T. Yang, L. Wang, J. Yao, B. Guo, Probing the unexpected behavior of AuNPs migrating through nanofibers: a new strategy for the fabrication of carbon nanofiber-noble metal nanocrystal hybrids nanostructures, Journal of Materials Chemistry A 2 (2014) 11174.
[42] H. Zhu, J. Zhang, R.Y. Zhang, M. Du, Q. Wang, G. Gao, J. Wu, G. Wu, M. Zhang, B. Liu, J. Yao, X. Zhang, When Cubic Cobalt Sulfide Meets Layered Molybdenum Disulfide: A Core-Shell System Toward Synergetic Electrocatalytic Water Splitting, Advanced Materials 27 (2015) 4475.
[43] H. Zhu, M. Zhang, S. Cai, Y. Cai, P. Wang, S. Bao, M. Zou, M. Du, In situ growth of Rh nanoparticles with controlled sizes and dispersions on the cross-linked PVA-PEI nanofibers and their electrocatalytic properties towards H_2O_2, RSC Advances 4 (2014) 794.
[44] Z. Zhu, Y. Su, J. Li, D. Li, J. Zhang, S. Song, Y. Zhao, G. Li, C. Fan, Highly sensitive electrochemical sensor for mercury(II) ions by using a mercury-specific oligonucleotide probe and gold nanoparticle-based amplification, Analytical Chemistry 81 (2009) 7660.
[45] X.X. Xu, G.T. Duan, Y. Li, G.Q. Liu, J.J. Wang, H.W. Zhang, Z.F. Dai, W.P. Cai, Fabrication of Gold Nanoparticles by Laser Ablation in Liquid and Their Application for Simultaneous Electrochemical Detection of Cd^{2+} Pb^{2+}, Cu^{2+}, Hg^{2+}, ACS Applied Materials & Interfaces 6 (2014) 65.
[46] M.M. Hossain, M.M. Islam, S. Ferdousi, T. Okajima, T. Ohsaka, Anodic stripping voltammetric detection of arsenic(III) at gold nanoparticle-modified glassy carbon electrodes prepared by electrodeposition in the presence of various additives, Electroanalysis 20 (2008) 2244.
[47] H. Zhu, M.L. Du, M. Zhang, P. Wang, S.Y. Bao, L. Wang, J.M. Yao, Facile fabrication of AgNPs/(PVA/PEI) nanofibers: high electrochemical efficiency and durability for biosensors, Biosensors and Bioelectronics 49 (2013) 210.
[48] H. Zhu, M.L. Du, M. Zhang, P. Wang, S.Y. Bao, M.L. Zou, J.M. Yao, Self-assembly of various Au nanocrystals on functionalized water-stable PVA/PEI nanofibers: a highly efficient surface-enhanced Raman scattering substrates with high density of hot spots, Biosensors and Bioelectronics 54 (2014) 91.
[49] D. Zhao, X. Guo, T. Wang, N. Alvarez, V.N. Shanov, W.R. Heineman, Simultaneous Detection of Heavy Metals by Anodic Stripping Voltammetry Using Carbon Nanotube Thread, Electroanalysis 26 (2014) 488.
[50] H. Ma, R. An, L. Chen, Y. Fu, C. Ma, X. Dong, X. Zhang, A study of the photodeposition over Ti/TiO_2 electrode for electrochemical detection of heavy metal ions, Electrochemistry Communications 57 (2015) 18.
[51] H. Lin, M. Li, D. Mihailovič, Simultaneous Determination of Copper Lead, and Cadmium Ions at a $Mo_6S_{9-x}I_x$ Nanowires Modified Glassy Carbon Electrode Using Differential Pulse Anodic Stripping Voltammetry, Electrochimica Acta 154 (2015) 184.